

## Determination of Thermal Contact Resistances for Small TENV Electrical Machine

**Olfa MEKSI, Mohd Azri Hizami RASID, Alejandro OSPINA  
and Vincent LANFRANCHI**

Sorbonne University, University of Technology of Compiègne (UTC), EA 1006 Laboratory of  
Electromecanic, Centre of research Royallieu - 60319, Compiègne cedex, France  
Tel.: 33 (0)3442344234727, fax: 33 (0)344237937  
E-mail: meksiolf@utc.fr

*Received: 9 February 2016 /Accepted: 14 March 2016 /Published: 31 March 2016*

---

**Abstract:** In this paper, a thermal study of Synchronous Reluctant motor is proposed. A specific experimental method is applied in order to identify the thermal parameters, this method focus on the study of contact resistances and total thermal capacity. Generally, in the classical thermal modeling, the thermal contact resistance (TCR) is estimated by empirical values and the thermal capacities are calculated by analytical solutions. The originality of the proposed model is based on the complementarity between experimental procedure (machine at rest), thermal modeling and model reduction technique in order to determine these important parameters and validate results (thermal contact resistances and capacities). *Copyright © 2016 IFSA Publishing, S. L.*

**Keywords:** Electrical machine, Thermal modeling, Thermal contact resistance, Identification method, Experimental analysis.

---

### 1. Introduction

In the context of automotive industry, the use of electric and electronic equipment is rapidly growing in the last decades. Many efforts have been devoted by car manufacturers to electrify some vehicle functions, as the traction, assisted steering or clutch. A critical problem when designing and optimizing the electric machines used in these applications is related to predict accurately the thermal behavior.

Extract a thermal model is a difficult task because that takes into account many factors: complex machine geometry, heterogeneous components and different modes of heat transfer. A small Synchronous Reluctance (Synchrel) Totally Enclosed Non-Ventilated (TENV) prototype machine [1] is thermally analyzed in this article. In order to make a thermal

modeling of this machine, a novel experimental procedure is proposed. This procedure combines experimental results and two different Lumped Parameters (LP) models (reduced and detailed) in order to identify the thermal capacities of the machine and the contact thermal resistances in the motor.

The Lumped Parameters (LP) method was adopted by his effectiveness (accuracy and rapidity). The detailed model [2] includes the thermal conduction resistances (metallic parts), the convection thermal resistances (airgap, lateral cavities and end windings), the thermal contact resistances and the external thermal resistance between frame's machine and environment. Thermal capacities are also associated to each part to simulate transient behavior of the machine.

## 2. Machine Structure and Thermal Model

The studied machine is the Synchronous Reluctant machine prototype (Synchrel) that it was designed in LEC laboratory [2] (Fig. 1). It is a small Totally Enclosed Non-Ventilated (TENV) machine. The rotor is composed by a central aluminum piece than support the four rotor teeth. The stator is composed of a magnetic yoke, twelve slots and the same quantity of teeth.

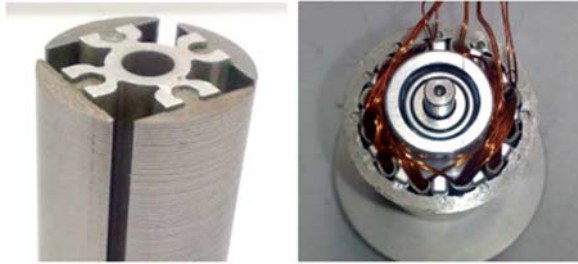


**Fig. 1.** Rotor and the completed assembly of the Synchrel machine prototype.

As can be seen in Fig. 2, the Synchrel machine studied has a relatively compact dimension: the length of the machine being far superior compared to its diameter. Thus, the radial surface is bigger than the axial surface. The end-windings are small compared with the total axial length, therefore, the end-windings and the active part of the windings inside the stator slot can be considered as a unified structure. The heat

evacuation through radial direction over the active length is then considered as the main heat evacuation path for all the heat produced by the machine.

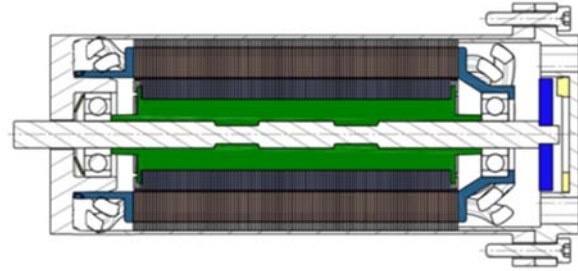


**Fig. 2.** Structure of the studied synchrel machine.

This Synchrel machine can support a maximal temperature  $T_{max}=120$  °C in windings. The stator is composed of a magnetic yoke, twelve slots and the same quantity of teeth. The electrical resistance of each phase is 0.22  $\Omega$ .

The thermal model is made using LP method: the geometry of the elementary parts was simplified into several blocks (cylindrical or cuboid shapes). As it is shown in Fig. 3, the different parts presented in a cross section are: the casing, the stator yoke, the stator teeth, the windings (windings, insulation and air), air gap, rotor and shaft. Additionally, in the axial direction, other blocks are considered: end-windings, cavities and frame (lateral caps). Then using thermal-electric analogy, the heat transfer in each block is represented by an equivalent electrical circuit [3].

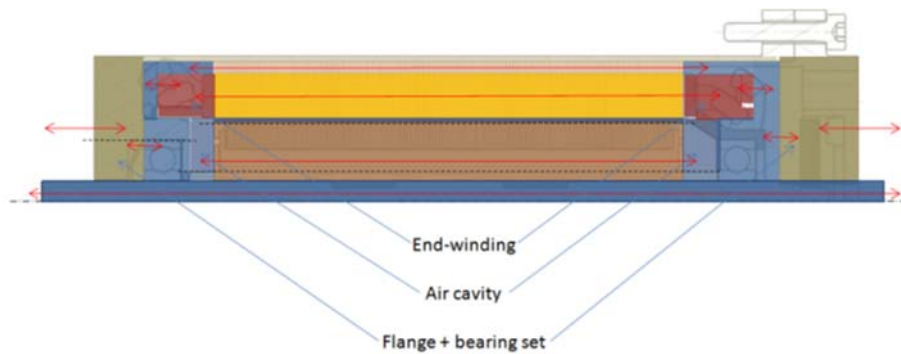


**Fig. 3.** Axial heat transfer including the end winding, air cavity and the flange and ball bearing set as elementary parts. In each elementary part, a resistance representing the elements thermal resistance is calculated.

In order to make the thermal model, three principal assumptions are made:

- 1) The different components of the motor are treated as; simple cylindrical or cuboid shapes;
- 2) The axial heat transfer is not considered except for frame and windings;
- 3) Due to the machine's symmetry, the model is done on an angular aperture corresponding to the quarter of the machine.

Over each bloc a thermal resistance is determined using the heat equation associated to each heat mode transfer. This resistance is defined by

$$R = \frac{\Delta T}{P}, \quad (1)$$

where  $\Delta T$  is the temperature gradient between two opposite surfaces of the shape and  $P$  is the heat

produced or crossing the block.  $P$  is related to the heat flow  $\vec{q}$  by the following equation,

$$P = \int_S q ds, \quad (2)$$

where  $S$  is the normal section traversed by  $\vec{q}$ .

Each heat transfer mode is associated with a thermal resistance as follow:

- for convection,

$$R_c = \frac{1}{h_c S}, \quad (3)$$

- for radiation,

$$R_r = \frac{1}{h_r S}, \quad (4)$$

- for conduction,

$$R_{c,cuboid} = \frac{L}{\lambda S}, \quad (5)$$

in these last three equations,  $S$  represent the cross section of an elementary block and  $h_c$ ,  $h_r$  are respectively the convection and radiation heat transfer coefficients and  $\lambda$  is the thermal conductivity. In the case of a cylindrical block shape, the conduction thermal resistance is defined by,

$$R_{c,cylinder} = \frac{1}{2\pi\lambda L} \ln\left(\frac{r_2}{r_1}\right), \quad (6)$$

where  $L$  is the axial length,  $r_1$  and  $r_2$  are the interior and exterior radius of the cylindrical block respectively.

Finally, to model the transient phenomena, thermal capacities should be present and associated to each section. These capacities represent the heat stored; they are defined by the following equation,

$$C_{th} = \rho c_p V, \quad (7)$$

where  $\rho$  is the density of the block material,  $c_p$  is its specific heat capacity and  $V$  is the block volume. The detailed thermal model obtained is showed in Fig. 4.

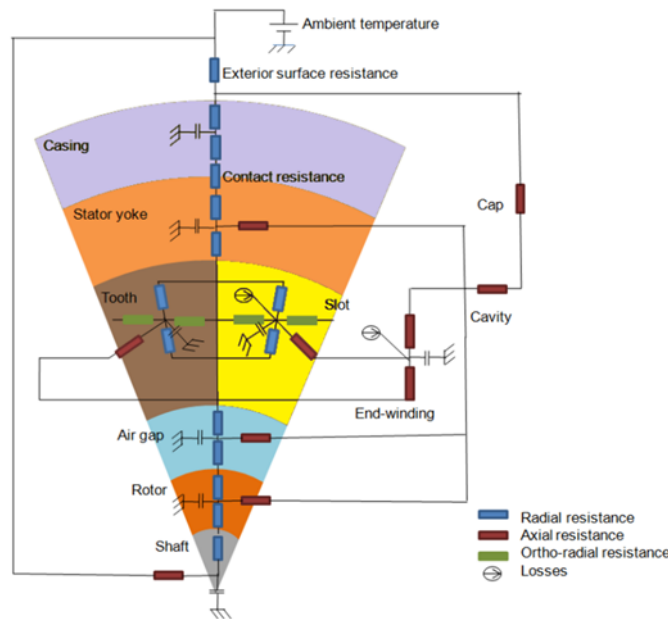


Fig. 4. Detailed Lumped parameters model of the Synchrel machine.

The major difficult about this thermal modeling is related to the accuracy of the heat transfer coefficients  $\lambda$ ,  $h_c$  and  $h_r$ . Many approaches are proposed in the literature. In the next subsections, the approaches used to find these heat transfer coefficients are presented.

### 2.1. Convection Coefficient

The convection represents the principal heat transfer in the air blocks (air-gap, cavities and external

environment). However, the distance between end-windings and frame is very small compared with other lengths; thus, the heat transfer is considered basically made by conduction. In the other cases (air-gap and external environment) the calculation of the convective heat transfer function requires a prior knowledge of the coolant (air) state. This calculation can be based on numerical methods, analytical analysis or empirical correlations. In all cases a dimensionless analysis is employed, this approach synthesizes the various thermal and mechanical

phenomena by grouping them into dimensionless numbers.

The heat transfer coefficient is calculated using these numbers, for example

$$h_c = \frac{\text{Nu} \cdot L_c}{\lambda}, \quad (8)$$

where Nu is the adimensionnel number comparing the convective heat transfer with the heat transfer by diffusion (conduction).  $L_c$  is the characteristic length.

In our case, the convection heat transfer between the machine surface and the environment is the most important mechanism and the only way to evacuate heat flux outside the machine. It could be affected by many factors as the position of the machine, its geometry, ambient temperature and even present bodies in its environment. These factors make it difficult to be characterized with accuracy.

In this study, a thermal analysis was done to determine the average natural convection heat transfer coefficient. A 3D numerical solution based on Computational Fluid Dynamics (CFD) is validated experimental measurements for validation and adopted [4].

For the airgap, a correlation extracted by physical analysis of the different phenomena was proposed by P. Teertstra, *et al.* [5], is used to evaluate the Nusselt number,

$$\text{Nu} = \frac{2\pi}{\ln(r_2/r_1)} + \left\{ \left[ \frac{1.028 \cdot F_{pr} \cdot \text{Ra}^{1/4}}{\left(1 + (r_1/r_2)^{3/5}\right)^{5/4}} \right]^2 + \left[ \frac{1}{720\pi^4} \cdot \frac{(r_2/r_1)}{(1 + r_2/r_1)} \cdot \text{Ra} \right]^2 \right\}^{-1/2}, \quad (9)$$

where  $Ra$  is the adimensionnel number comparing the gravitational with the viscous forces,  $F_{pr}$  is the constant, function of Prandtl number  $Pr$ ,

$$F_{pr} = \frac{0.67}{\left[1 + (0.5/Pr)^{9/16}\right]^{4/9}} \quad (10)$$

Before applying this correlation, it must that the thickness of the air gap must be very small comparing to the length of the machine which is the case for the Synchrel machine.

Using the numerical heat transfer coefficient for external natural convection and empirical results for the air gap, thermal convection resistances are calculated using Eq. (3).

## 2.2. Radiation

It represents the exchange of heat transfer by the emission of electromagnetic waves between solid blocs, for example, between rotor and stator inside the machine, or between the frame and other bodies. In this model, the radiation heat transfer is neglected

inside the machine, although, it is incorporated with the external convective heat transfer. Its representative resistance is defined by Eq. (4). The radiation coefficient is defined as follow

$$h_r = \varepsilon \sigma (T_s + T_a)(T_s^2 + T_a^2), \quad (11)$$

where  $\varepsilon$  is the emissivity coefficient depending on the material of each surface of the machine.  $\sigma$  is Stefan-Boltzmann constant equal to  $5.67 \times 10^{-8} \text{ W/m}^2/\text{K}^4$ .

In order to define the radiation coefficient, it's important to determine the emissivity for different frame surfaces of the machine. This task was done experimentally as it is described in Section 4.

## 2.3. Conduction

It represents the heat transfer mode within solid blocs. It's characterized by the thermal conductivity which is a thermophysical property of the material. For each part of the machine, values of this property are proposed in literature.

A model of two resistances (Eq. (5) and Eq. (6)) for circumferential and radial transfer is associated to windings and teeth. From the slot to the both stator yoke and air gap, a single thermal contact resistance is used (for radial direction). In this equivalent thermal model, the axial transfer is not considered only for the frame (radial surface >> axial surface).

In the ideal case, the heat flow is conducted through the contact surface between two solid blocs with any changes in temperature, a more realistic model need to consider thermal contact resistance. That requires close viewing of this phenomenon and understanding of the different approaches proposed in literature.

## 3. Thermal Contact Resistances

The thermal behavior at the contact surface between two solids is a complex phenomenon. The contact surface has imperfections like very small gaps (interstitial cavities) due to roughness or machining, material hardness and smoothness of surfaces (see Fig. 5) [6]. The assembly method can too affect the heat flow: interface pressure, and air pressure. The interstitial cavities contain air and residual impurities, so, it is not evident to identify its nature and thickness. Recent studies showed that the values of thermal contact resistances are affected not only by shrink fit pressure and surface properties but also by heat flux and temperature [7-8].

These imperfections are represented by thermal contact resistances which causes a temperature difference established by these imperfections (Fig. 6). The leading method of determining this thermal contact resistance is based on the equivalent properties (equivalent typical length and equivalent thermal conductivity).

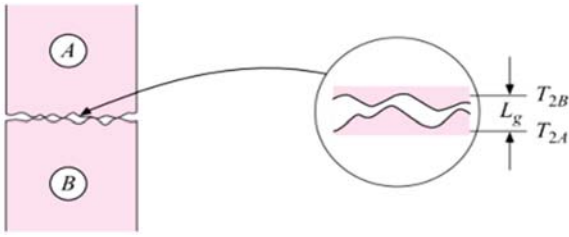


Fig. 5. Schematic of an imperfect contact between two solids.

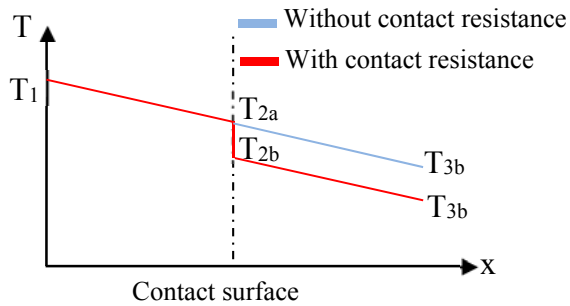


Fig. 6. Temperature variation through a contact surface with and without contact resistance.

For contact between bare geometries (concentric cylinders, two plate surfaces), models are proposed in literature. Analyses on these models allowed concluding that they overestimate the thermal contact resistance with considerable error [7-8].

Generally, in the thermal model of electrical machines, the contact between different blocs is considered perfect. But the fact that the air's thermal conductivity confined in the pockets is lower than thermal conductivity of solid blocs implies that this contact should be taken into account. The sensitivity analysis done in [9] asserts that the thermal contact resistance is among the significant parameters. Besides, it was demonstrated that the variation of this parameter by some micrometers can affect the model temperature. As a result, the accuracy of the thermal model is related to a correct estimation of these contact resistances (besides other aspects) [10-11].

Typical values of thermal contact resistance [ $m^2C/W$ ] and thermal contact conductance between typical surfaces used in electric machines are given in some textbooks on heat transfer [3, 6]. To build the thermal model, Anderson [9] used these values. On the other side, Staton and al. [10] compared their experimental results to the proposed results in literature for thermal contact resistance of lamination to housing gap and an important difference was found.

Trying to obtain values for thermal contact resistances between stator and housing assuming that it depend just on the initial shrink fit pressure, Devdatta, *et al.* [13] designed a series of experiments on nine different prototypes of Water Cooled Jacket for Electrical machines with different shrink fit

pressure. In some cases, it's difficult to compare to these results, because not enough information is provided about heat flux and machine dimensions.

Trigeol, *et al.* [14] used literature as reference for the first estimation of the different contact resistances (frame-stator, stator-winding) despite the variety of proposed values. Then, assuming that thermophysical properties of materials are homogenous and known with accuracy and determining convective heat transfer coefficient experimentally, calibration with experimental results was introduced. This method is considered still indispensable for some authors [12].

Finally, we should indicate that for contact between stator and winding, the dominant method is the homogenization which regroups the contact between conductors and resin and between winding and the stator yoke [2, 15].

In our case, a sensitivity analysis allowed us to conclude the more influential thermal contact resistances.

#### 4. Experimental Analysis

The machine housing is constituted by three different surfaces: a smooth cylindrical surface with some complexity in sides, a lateral irregular surface and a square lateral surface as is shown in Fig. 7.

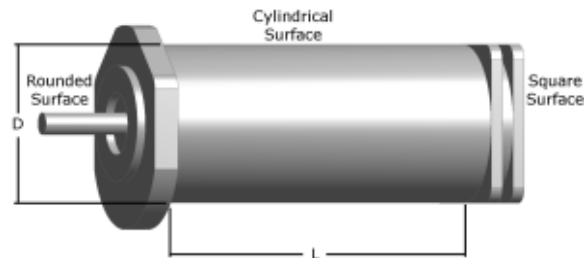


Fig. 7. Synchrel motor housing shape.

The experimental analysis was achieved in two steps. In the first, the machine frame was insulated with polyurethane foam (external environment) for parameters identification. In the second step, the polyurethane foam is removed and results are used for results validation. In both steps, the machine was heated using a DC test (at rest). Five thermocouples (type k) have been used to survey the frame, windings, polyurethane foam and ambient temperature.

The experimental set-up is schematically described in Fig. 8. The Synchrel machine is hanged inside a closed test cabin. It serves to limit two major kind of external perturbations: external bulk fluid movements and external heat sources due to radiation. Besides, the internal surface of the test cabin was painted in black in order to reduce the internal reflected radiation. The dimensions of the test cabin were chosen so that don't affect experimental results and keep a stable ambient

temperature. The emplacements of the five thermocouples are shown in Fig. 8: one is placed in a perforated notch over the cylindrical surface (point 1), the two others were placed in the windings (points 2 and 3) and the last one was placed on the polyurethane foam when it was used. The ambient temperature was measured by a thermocouple placed at the bottom corner inside the test cabin (point 4).

An infrared camera, placed in a viewing window, measures the emissivity of each machine's surface. It was determined experimentally using a black adhesive as a reference, with a known emissivity: the emissivity parameter of the infrared camera was adjusted so that the temperature at a point in the vicinity is equal to the temperature measured over the black adhesive.

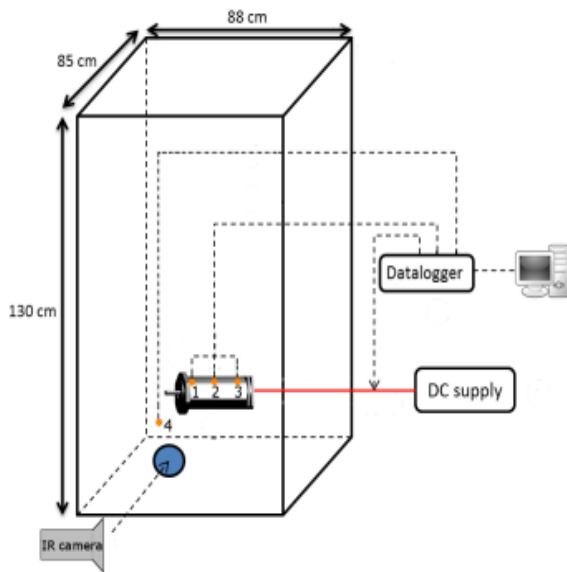


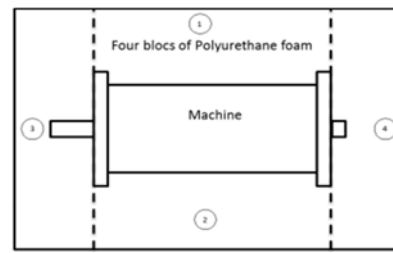
Fig. 8. Experimental set-up.

In the first step, the experimental procedure consists to totally insulate the external surface using an insulating material (polyurethane foam). So, a set of insulation blocks were designed to insulate different outer shapes of the machine (see Fig. 9). In this case, an additional thermocouple was positioned to measure the temperature at this material.

The obtained winding and frame temperatures evolution, in adiabatic conditions are shown in Fig. 10. At this stage, the thermal contact resistances are determined in a purpose of fitting experimental and detailed model results in adiabatic conditions.

Besides, this procedure allows us to determine the parameters of the second order thermal model presented in Fig. 11.

Using two experimental measurements  $T_w$  (winding temperature) and  $T_{amb}$  (ambient temperature), by fitting, it's possible to determine  $R_{int}$  and  $C_{int}$  (internal thermal resistance and capacity representing the internal heat storage and transfer) and  $R_{ext}$  and  $C_{ext}$  (external thermal resistance and capacity representing the external heat storage and transfer).



(a) Insulation blocks



(b) 1 and 2

(c) 3

(d) 4

Fig. 9. Insulation blocs: disposition and photographies.

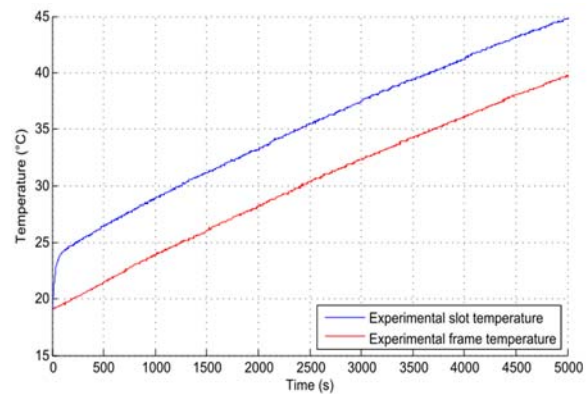


Fig. 10. Experimental evolution of the frame and winding temperature in adiabatic conditions.

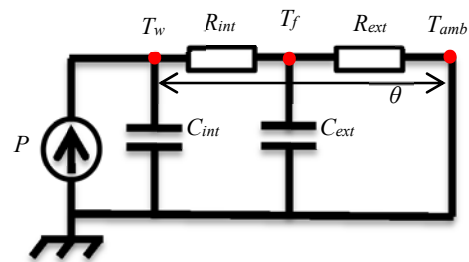


Fig. 11. Simplified thermal model of the whole machine.

In comparison with the ambient temperature, the evolution  $\theta(t)$  is considered like a second order function, described by Eq. (12).

$$\begin{aligned}
 P &= C_{int} \frac{d\theta_i}{dt} + \frac{1}{R_{int}} (\theta_i - \theta_e), \\
 0 &= C_{ext} \frac{d\theta_e}{dt} + \frac{1}{R_{int}} (\theta_e - \theta_i) + \frac{1}{R_{ext}} \theta_e,
 \end{aligned} \tag{12}$$

where  $\theta_i$  is the gradient temperature between the windings and the frame and  $\theta_e$  is the gradient temperature between the frame and ambient.

The Laplace transform of the solution of this equation is in the formula of Eq. (13)

$$\theta = \theta_{RP} (1 - Ae^{-t/\tau_1} - Be^{-t/\tau_2}), \quad (13)$$

where  $\theta_{RP} = PR_{tho}$  and  $R_{tho} = R_{int} + R_{ext}$ .

In this analysis, the heat transfer inside and outside the machine is represented by internal and external thermal capacities and resistances. The windings are considered as the heat source and fixed at the measured windings temperature. The frame's temperature is considered homogeneous and fixed at the frame's temperature. The stored heat and the heat transfer are presented by  $C_{int}$  and  $R_{int}$ , respectively. The heat is dissipated into external environment (insulating foam), then an external thermal resistance  $R_{ext}$  between the machine's frame and the ambient air is used to represent the heat transfer inside the insulating foam (thermal conduction).

In this way, the constants are defined by  $A = R_{ext}/R_{tho}$ ,  $B = R_{int}/R_{tho}$ ,  $\tau_1 = R_{ext}C_{ext}$  and finally  $\tau_2 = R_{ext}C_{int}$ . These constants are calculated by fitting experimental curves when the machine is totally insulated. All parameters are then deduced from  $A$  and  $B$  knowing the injected Joule losses  $P$ . The external resistance is used in the detailed model with the corresponding injected Joule losses. Thermal parameters are compared with which was calculated analytically.

The second step, when the insulation is removed, the experimental results are used to validate the results of the detailed model using the proposed thermal contact resistances values.

## 5. Identification Model: Contact Resistances

The thermal model of an electrical machine using the Lumped Parameters method is a network consisting of thermal resistances and capacities. In our study, this model is reduced to a second order model. This model allows us to calculate the parameters of the simplified model (Fig. 11).

For that several methods are proposed in the literature. Some are based on physical approach of thermal phenomena or sensitivity analyzes [10, 16-18]; others have conducted reduction model using mathematical approaches [19-20].

In our study, a mathematical approach is applied to the detailed thermal model of the machine. In addition, an experimental protocol is proposed to determine the total heat capacity and the external resistance.

Model reduction consists of replacing the state representation of any order by another with a lower order keeping the same input-output relationship. The

iterative methods were introduced from 1950 using the moment matching technique. These methods fall into two classes: explicit moment matching (asymptotic wave evaluation) and implicit moment matching (Padé via Lanczos, Padé via Arnoldi) which is more used in order reduction field [21].

The equivalent detailed thermal model is a network can be represented and described by the following system of differential equations (Eq. (14)) [22], applying the energy equation on each node [19, 23],

$$\dot{T} = -C_a^{-1}GT + C_a^{-1}\phi, \quad (14)$$

where  $T$  is the temperature vector (state vector),  $C_a^{-1}$  is the thermal capacitance matrix,  $G$  is the conductance matrix (obtained by inverting the resistance matrix) and  $P$  is the matrix containing all the thermal excitations (heat sources, boundary conditions).

In the interest of solving and reducing the thermal model of the machine, we use another formulation extracted from the Laplace transform and using complex matrices for the numerical calculation. First of all, the temperature of each node is expressed in comparison of the ambient temperature

$$\theta = T - T_{amb}. \quad (15)$$

Applying the Laplace transform to system (14) and using Eq. (15), formula (16) can be written:

$$s\theta = -C_a^{-1}G\theta + C_a^{-1}\phi, \quad (16)$$

from this representation, the matrix admittance containing the thermal conductance and capacities of the network, can be defined

$$Y(s) = G + C_a s, \quad (17)$$

so the obtained new formulation of the problem is,

$$\phi = Y(s)\theta, \quad (18)$$

This formulation assembles in one matrix all the information of both the static and dynamic regimes. The reduction operation is applied to it to approach the output with a reduced matrix  $Y_{red}(s)$  of the order  $p$ , much smaller than the order of the original representation (Fig. 12).

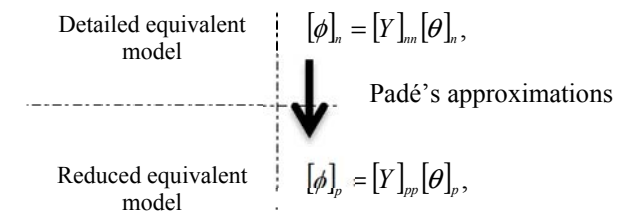


Fig. 12. Reduction of the detailed equivalent model.

In this study, the Padé's approximations are applied on the complex equivalent circuit. This moment matching technique utilizes an iterative algorithm to express the transfer function of the network as continued function.

To obtain this reduced thermal function, the experimental external thermal resistance  $R_{ext}$  is used in the detailed model to represent the conduction heat transfer phenomenon (representing the heat transfer via the foam of polyurethane). This procedure allows us to figure out the impact of the thermal contact resistances on the simplified model (obtained using Padé's approximations).

## 6. Sensitivity Analysis

A sensitivity study has been made to determine the most influential thermal contact resistances: shaft/rotor, windings/stator in either directions (radial and orthoradial) or stator/frame. Four cases are investigated: at each time, only a thermal contact resistance varies and others are Results are showed in Fig. 13.

The results of this study showed that the most influent thermal contact resistances are between the stator/frame and the stator/windings in the radial direction (in red) as it's shown in Fig. 14.

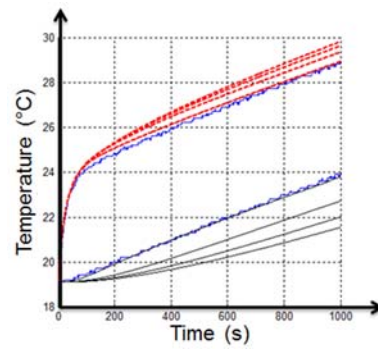
In our study, these resistances are used in the detailed model and the others are not considered (shaft/rotor and windings/stator in the orthoradial direction).

## 7. Results and Discussion

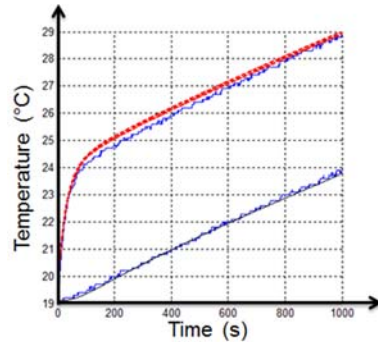
In the first experimental step (isolated machine), an analysis is effectuated in order to obtain the values of thermal contact resistances. It is supposed that the uncertainties related to thermal conduction and thermal convection (machine at rest, Nusselt number  $\approx 2$ ) are weakest compared to the uncertainties linked to contact thermal resistances. The thermal contact resistances are determined by identification. For the validation, results of the second experiment are used.

A comparison between experimental and model results (detailed model) for the insulated machine is shown in Fig. 15; in this comparison the contact resistances are annulated in the detailed model.

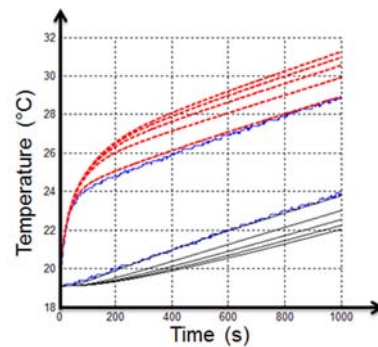
The results show an important deviation for frame temperature and a more slight deviation for slot temperature. Based on the sensitivity analysis, intervals for TCRs are fixed and used to determine the values that allow fitting the model to experimental results.



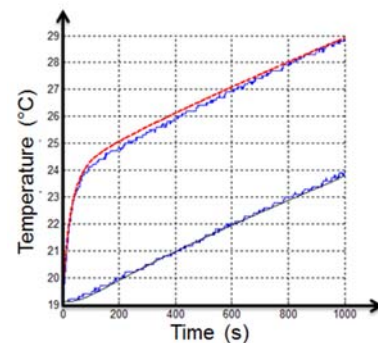
(a) Influence of the thermal contact resistance between stator yoke and frame.



(b) Influence of the thermal contact resistance between windings and teeth.



(c) Influence of the thermal contact resistance between windings and stator.



(d) Influence of the thermal contact resistance between shaft and rotor.

— Experimental slot temperature  
 — Experimental frame temperature  
 — Model frame temperature with thermal contact resistance  
 — Model slot temperature with thermal contact resistance

**Fig. 13.** Influence of each thermal contact resistance on the variation of model temperature.



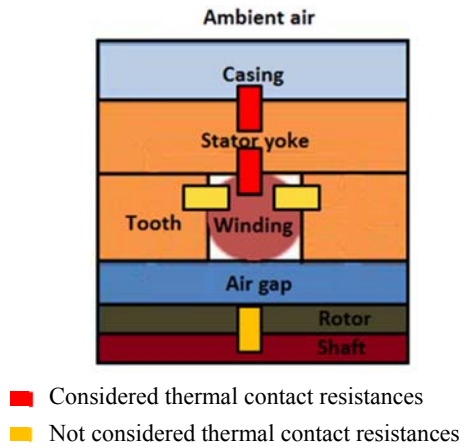


Fig. 14. Repartition of thermal contact resistances.

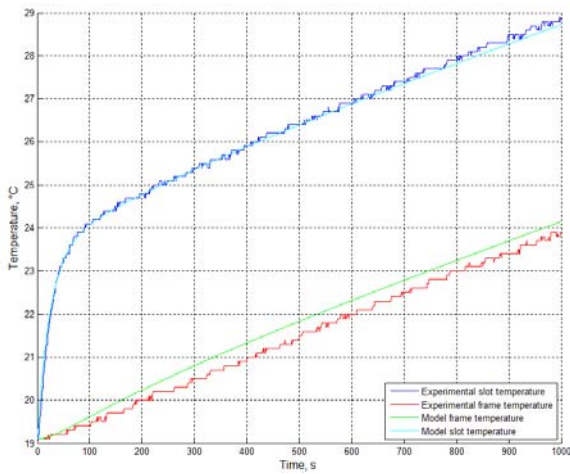
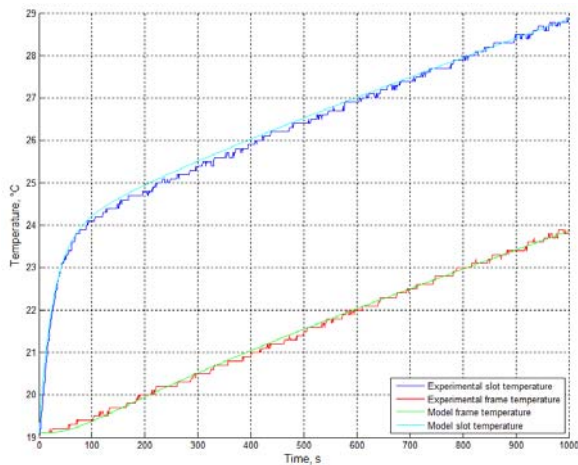
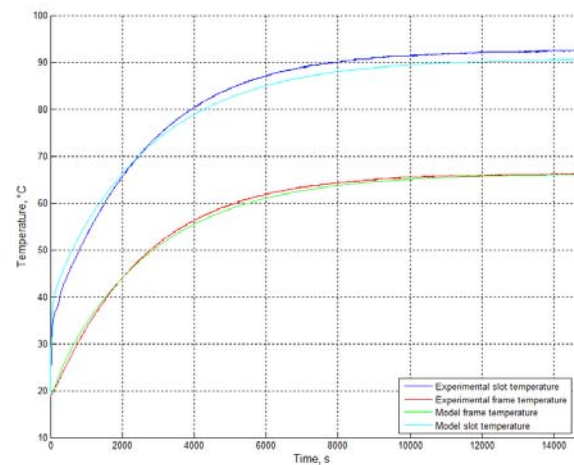


Fig. 15. Comparison between experimental and model results without contact resistances for insulated and not insulated machine.

The obtained thermal contact resistances allow obtaining the results showed in Fig. 16(a). For stator yoke/frame contact, the thermal conductance is equal



(a) Insulated



(b) Not insulated

Fig. 16. Comparison between experimental and model results with contact resistances for insulated and not insulated machine.

to  $W/m^2/^\circ C$ , it smaller than values proposed by Staton [11] and comparable with the results proposed by Trigeol [14]. For yoke/windings the obtained conductance is much higher with a value of  $60000 W/m^2/C$ , bigger than values proposed by Trigeol [14]. Results in Fig. 16(b) are showed to validate the obtained results (not insulated machine).

In order to make a more confident validation of thermal contact resistances, two simplified models (two nodes, see Fig. 11) are compared: the first is obtained by measures fitting and the other by model reduction (Padé's approximations) over the detailed model.

The fitting of experimental results are made using Eq. (13). Thus, the total thermal capacity and the external thermal resistance, between frame's machine and environment, as the internal parameters related to windings are computed. The results are resumed in Table 1. The external thermal resistance obtained by the experimental fitting and representing the heat transfer within the insulating polyurethane foam (conduction), is inserted in the detailed model.

The Padé's approximations are applied to obtain the reduced transfer function representing the detailed model, firstly, without thermal contact resistances (Padé (W.TCRs)). Using this transfer function,  $C_{ext}$ ,  $R_{ext}$ ,  $C_{int}$  and  $R_{int}$  are calculated (see Table 1). A big difference can be observed specially for internal parameters.

In the other side, the comparison between results of both experimental fitting and Padé's approximations applied over the detailed model with proposed thermal contact resistances values (Padé (TCR) in Table 1) shows coherence between the parameters. Thus, the estimation of TCRs is validated.

According to these results, it is concluded that the internal capacities in the detailed model are correctly calculated because the capacities obtained by reduction has a slight difference compared to experimental capacities (fitting).

**Table 1.** Comparison between the parameters of the reduced models considered and not considered the thermal contact resistances.

Method	Exp. (fitting)	Padé (TCRs)	Padé (W. TCRs)
$C_{ext}$ (W/K)	519.02	519.33	512.44
$R_{ext}$ (K/W)	30.94	30.94	30.94
$C_{int}$ (W/K)	17.02	19.56	26.86
$R_{int}$ (K/W)	2.10	2.51	1.94

## 8. Conclusion

In this paper, an experimental procedure is proposed in order to evaluate the thermal contact resistances. And an identification method is proposed to determine the parameters (internal and external thermal capacities and resistances) of a simplified thermal model of electrical machines. Then this simplified model is used to validate the proposed values of thermal contact resistances. These parameters were investigated for a small Totally Enclosed Not Ventilated (TENV) Synchrel motor. The experimental analysis is made in two stages: in the first, the machine was insulated and a dc test is done in order to estimate the parameters of the simplified model (experimental fitting). The same experiment was used to determine the TCRs by fitting detailed model and experimental results.


A model reduction technique (Padé's approximations) was applied on the detailed model, then, the parameters identification allowed to compare the experimental fitting with the analytical results. The difference is found important when the TCRs are not considered and negligible in the other case, which validate the proposed values for TCRs. Comparing to results proposed in literature, an important difference was found. These variety and dispersion in values can be due to the fact that these resistances are depending upon the manufacturing process and used materials.

## References

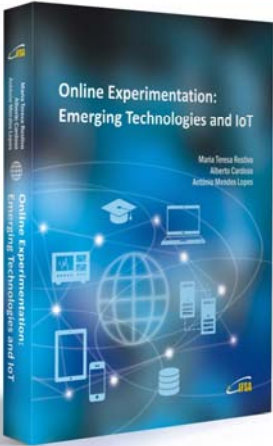
- [1]. C. Doc, Contribution à la conception et au dimensionnement d'un actionneur d'embrayage, PhD Thesis, *University of Technology of Compiègne*, 2010.
- [2]. M. A. H. Rasid, A. Ospina, K. El Kadri Benkara, *et al.*, Thermal model of stator slot for small synchronous reluctance machine, in *Proceedings of the IEEE International Conference on Electrical Machines (ICEM)*, 2014, pp. 2199-2204.
- [3]. F. P. Incropera, T. L. Bergman, *et al.*, Fundamentals of heat and mass transfer, *John Wiley and Sons*, 2011.
- [4]. Meksi Olfa, Vargas Alejandro Ospina, Numerical and experimental determination of external heat transfer coefficient in small TENV electric machines, in *Proceedings of the IEEE Energy Conversion Congress and Exposition (ECCE)*, 2015, pp. 2742-2749.
- [5]. K. N. Srinivas, R. Arumugam, Thermal characterization through finite element analysis of the switched reluctance motor, in *Proceedings of the IEEE Region 10<sup>th</sup> International Conference on Electrical and Electronic Technology (TENCON'01)*, Vol. 2, 2001, pp. 819-823.
- [6]. J. P. Holman, Heat transfer, Eighth SI Metric Edition, *McGraw-Hill Inc.*, 2001.
- [7]. R. Camilleri, Howey David, McCulloch M. D., *et al.*, Experimental investigation of the thermal contact resistance in shrink fit assemblies with relevance to electrical machines, in *Proceedings of the 7<sup>th</sup> IET International Conference on Power Electronics, Machines and Drives (PEMD)*, 2014, pp. 1-9.
- [8]. P. H. Mellor, D. Roberts, D. R. Turner, Lumped parameter thermal model for electrical machines of TEFC design, *IEE Proceedings B (Electric Power Applications)*, *IET Digital Library*, Vol. 138, No. 5, 1991, pp. 205-218.
- [9]. C. V. Madhusudana, Thermal conductance of cylindrical joints, *International Journal of Heat and Mass Transfer*, Vol. 42, No. 7, 1999, pp. 1273-1287.
- [10]. B. Andersson, Lumped Parameter Thermal Modelling of Electric Machines, PhD Thesis, *Chalmers University of Technology*, Göteborg, Sweden, 2013.
- [11]. D. Staton, A. Boglietti, A. Cavagnino, Solving the more difficult aspects of electric motor thermal analysis, in *Proceedings of the IEEE Electric Machines and Drives Conference*, Vol. 2, 2003, pp. 747-755.
- [12]. C. Vasilescu, Modélisation du transfert de chaleur au sein des machines électriques tournantes: dimensionnement et optimisation de leur système de refroidissement, Doctoral Dissertation, *Université Pierre et Marie Curie*, Paris, 2002.
- [13]. P. K. Devdatta, G. Rupertus, E. Chen, Experimental investigation of contact resistance for water cooled jacket for electric motors and generators, *IEEE Transactions on Energy Conversion*, Vol. 27, No. 1, 2012, pp. 204-210.
- [14]. J. Trigeol, Identification des pertes d'une machine électrique par une approche thermique et à l'aide d'une technique inverse, PhD Thesis, *Université de Poitiers*, 2004.
- [15]. J. Driesen, R. J. Belmans, K. Hameyer, Finite-Element Modeling of Thermal Contact Resistances and Insulation Layers in Electrical Machines, *IEEE Transactions on Industry Applications*, Vol. 37, No. 1, 2001, pp. 15-20.
- [16]. J. Lindström, Thermal model of a permanent-magnet motor for a hybrid electric vehicle, Research Report, *Dept. of Electric Power Eng., Chalmers University of Technology*, Göteborg, Sweden, 1999.
- [17]. R. Khliissa, Contribution à la définition des méthodes d'optimisation rapides et économiques pour le dimensionnement d'actionneurs électriques, PhD Thesis, *University of Technology of Compiègne*, 2015.
- [18]. B. Assaad, Contribution à la prise en compte des aspects thermiques des machines électriques dans un environnement mécatronique, PhD Thesis, *University of Technology of Compiègne*, 2015.
- [19]. N. Jaljal, J. F. Trigeol, P. Lagonotte, Reduced Thermal Model of an Induction Machine for Real-Time Thermal Monitoring, *IEEE Transactions on Industrial Electronics*, Vol. 55, No. 10, 2008, pp. 3535-3542.
- [20]. M. Broussely, Réduction de modèles thermiques par la théorie des réseaux, application à la surveillance d'une machine asynchrone par couplage de modèle thermique réduit avec un schéma équivalent électrique, PhD Thesis, *Université de Poitiers*, 2000.

- [21]. A. Davoudi, Reduced-order modeling of power electronics components and systems, PhD Thesis, *University of Illinois at Urbana-Champaign*, 2010.
- [22]. P. Feldmann, R. W. Freund, Efficient linear circuit analysis by Padé approximation via the Lanczos process, *IEEE Transactions on Computer-Aided Design of Integrated Circuits and Systems*, Vol 14, 1995, pp. 639-649.
- [23]. M. Broussely, Y. Bertin, P. Lagonotte, Reduction and optimization of thermal models using Kirchhoff network theory, *International Journal of Thermal Sciences*, Vol. 42, No. 8, 2003, pp. 795-804.
- [24]. O. Meksi, M. A. H. Rasid, A. Ospina Varga, V. Lanfranchi, Experimental investigation of contact resistances for small TENV electrical machine, in *Proceedings of the International Symposium on Electromagnetic Fields*, September 2015.

2016 Copyright ©, International Frequency Sensor Association (IFSA) Publishing, S. L. All rights reserved.  
(<http://www.sensorsportal.com>)



## Online Experimentation: Emerging Technologies and IoT



**Maria Teresa Restivo, Alberto Cardoso, António Mendes Lopes (Editors)**

*Online Experimentation: Emerging Technologies and IoT* describes online experimentation, using fundamentally emergent technologies to build the resources and considering the context of IoT.

In this context, each online experimentation (OE) resource can be viewed as a "thing" in IoT, uniquely identifiable through its embedded computing system, and considered as an object to be sensed and controlled or remotely operated across the existing network infrastructure, allowing a more effective integration between the experiments and computer-based systems.

The various examples of OE can involve experiments of different type (remote, virtual or hybrid) but all are IoT devices connected to the Internet, sending information about the experiments (e.g. information sensed by connected sensors or cameras) over a network, to other devices or servers, or allowing remote actuation upon physical instruments or their virtual representations.

The contributions of this book show the effectiveness of the use of emergent technologies to develop and build a wide range of experiments and to make them available online, integrating the universe of the IoT, spreading its application in different academic and training contexts, offering an opportunity to break barriers and overcome differences in development all over the world.

*Online Experimentation: Emerging Technologies and IoT* is suitable for all who is involved in the development design and building of the domain of remote experiments.

**Hardcover: ISBN 978-84-608-5977-2**  
**e-Book: ISBN 978-84-608-6128-7**

**Order: [http://www.sensorsportal.com/HTML/BOOKSTORE/Online\\_Experimentation.htm](http://www.sensorsportal.com/HTML/BOOKSTORE/Online_Experimentation.htm)**